Sensors and Materials, Vol. 23, No. 5 (2011) 251–261
MYU Tokyo

S & M 0843

Liquid-Phase Formation of Silver Nanoparticles on a Glass Substrate Regulated by Gold Nanoparticles

Kohei Hanada, Kazuhiro Uchida, Daniel Citterio and Norihisa Miki*

Keio University, 3-14-1 Hiyoshi, Kohoku-ku, Yokohama, Kanagawa 223-8522, Japan

(Received February 1, 2010; accepted August 16, 2010)

Key words: nanoparticle, liquid-phase reduction, silver nanoparticle, gold nanoparticle, fluorescence enhancement

In this paper, we demonstrate the formation of uniformly distributed silver nanoparticles (NPs) regulated by gold NPs deposited in advance, and demonstrate their application to the enhancement of fluorescent signals. First, gold NPs were created by liquid-phase citrate reduction, and preferentially deposited onto surfaces chemically modified with 3-aminopropyl-trimethoxysilane (APTS). After the APTS was removed by oxygen plasma treatment, silver NPs were deposited onto the glass surface by a modified silver mirror reaction. Distribution of the silver NPs formed on the substrate was controlled by the reaction times of the gold and silver NP reduction processes. With gold NPs present, the silver NPs were more likely to deposit as isolated NPs than as aggregated NPs. This enabled the gold/silver NP substrates to achieve a significantly enhanced rhodamine-6G fluorescence, 8 times greater than that of a glass substrate on average, and greater than those of substrates with only silver or only gold NPs. The proposed gold and silver nanoparticle substrates are readily applicable to ultrasensitive bio/chemical detection technology.

1. Introduction

Metal nanoparticles (NPs) have been extensively studied for various uses, such as ultrasensitive bio/chemical detection using fluorescence enhancement[1–6] and/or surface-enhanced Raman scattering.[7–13] Silver NPs are known to exhibit high enhancement whereas gold NPs have been widely used owing to their chemical stability and affinity to biochemical substances. They are also highly efficient catalysts because of their extremely large surface/volume ratio.[14–18] These characteristics of NPs depend on the metal species and the nanoscale geometry.

Because metal NPs are 10–100 nm in size, bottom-up techniques such as liquid-phase reduction[19–25] and Langmuir-Blodgett patterning[26–28] are more attractive than top-down techniques such as photolithography and e-beam lithography, owing to shorter

*Corresponding author: e-mail: miki@mech.keio.ac.jp

process times and lower costs. In particular, liquid-phase reduction is a low-temperature (below 100°C), low-vacuum process suitable for the low-cost manufacture of metal NPs. Citrate reduction of gold chloride is one of the most frequently used techniques for forming gold NPs, which are used to manufacture a highly conductive metal layer[19] and for ultrasensitive biochemical analysis.[20–22] Citric acid not only reduces gold but also coats the surfaces of the formed gold NPs, preventing the NPs from aggregating to form large particles or films. Silver NPs can be formed by reducing silver nitrate.[23-25] A modified silver mirror reaction, in which dispersants are added to a conventional silver mirror reaction, can deposit silver NPs ~ 30 nm in diameter onto a glass substrate.[25] This process can be combined with the spatial surface modification of the glass substrate by microcontact printing of a self-assembled monolayer (SAM), which enables site-selective deposition of silver NPs. Techniques for combining several different metals on the nanometer scale have been proposed, in relation to the fabrication of alloy metal nanostructures,[29–31] deposition of metal NPs onto substrates with a different metal layer,[32,33] or localized spontaneous galvanic displacement reactions.[34] Previous reports suggest that multicomponent surface compositions produce synergistic effects and augment their activities.

It was reported that the nanostructures of metal NPs strongly affected the enhancement of fluorescence signals (SEF) and Raman signals (SERS)[1–13,20–22,25] though the mechanisms of SEF and SERS are not yet conclusive. This work is dedicated to demonstrate a bottom-up manufacturing process of silver and gold NPs that can regulate the formation of silver NPs by gold NPs deposited in advance. First, we deposited citrate-reduced gold NPs onto a glass substrate covered with 3-aminopropyl-trimethoxysilane (APTS) (Wako Chemicals). Gold NPs were deposited onto the surfaces with an interaction between the citric acid on the gold NPs and amino terminal groups of the APTS SAM. The density of gold NPs was proportional to the reaction time. Then, the substrate was treated with oxygen plasma to remove the SAM and expose the glass surface, upon which silver NPs were formed in the subsequent modified silver mirror reaction. Silver NPs were more likely to deposit as isolated NPs, rather than as aggregates, in the presence of gold NPs with appropriate densities. The formed silver/gold NP substrates exerted greater fluorescence enhancement than glass substrates by a factor of 8 and silver NP substrates by a factor of 2 when the deposition of silver and gold NPs was properly controlled.

The proposed bottom-up process of forming gold and silver NPs on a glass substrate, which do not require high vacuum or high temperature, is readily applicable to ultra-sensitive bio/chemical detection and highly efficient catalytic reaction.

2. Materials and Methods

2.1 *Deposition of metal NPs*

2.1.1 *Deposition of gold NPs*

Gold NPs were formed by citrate reduction from chloroauric acid (HAuCl4) solution, as proposed previously.[19–22] A 100 mL sample of 0.75 mM $HAuCl_4 \cdot 4H_2O$ (Wako Chemicals) was brought to a vigorous boil while being stirred, and 4.5 mL of 0.13 M

sodium citrate (Wako Chemicals) was rapidly added to the solution, which was then boiled for 20 min. Sodium citrate reduces gold and also functions as a dispersant. The solution was cooled to room temperature with continued stirring. The suspension was filtered using a 2-μm-pore-size syringe filter, and stored in the refrigerator until further use.

To deposit gold NPs, the glass substrate surfaces were covered with a SAM having amino terminal groups. The glass substrate surface was cleaned with an oxygen plasma (SAMCO, Compact Etcher FA-1) at 100 W for 5 s prior to the modification. It was then derivatized with APTS (Wako Chemicals) by immersing it in 1% anhydrous toluene solution (Wako Chemicals). After 5 min, it was removed and rinsed with ethanol (Wako Chemicals, 99.8%). After drying under N_2 gas, it was subsequently heated to 120°C for 5 min to enhance the APTS adsorption. Then, it was rinsed twice in ethanol and DI water with sonication for 5 min to remove unbound silanizing reagent from the surface. After drying under N_2 gas, the substrate was immersed in the gold NP solution to form a monolayer of gold NPs on the glass surface, with the citric acid groups on the gold NPs bound to the amino terminal groups of the APTS by ionic interaction. Depending on the immersion time and concentration of the gold NP solution, gold NP layers with various interparticle distances were formed on the glass.

2.1.2 *Deposition of silver NPs*

We fabricated silver NPs using a modified silver mirror reaction, in which dispersants were added to a conventional silver mirror solution (silver nitrate solution + ammonia solution) as in our group's previous report.[25]

The glass substrate surface was cleaned using an oxygen plasma at 50 W for 60 s prior to the modified silver mirror reaction. Ammonia solution (Wako Chemicals, 5.7%, 8 mL), DI water (20 mL), and the dispersant (BYK Additives & Instruments, Disperbyk-102, 1.5 mL) were added to a silver nitrate solution (Wako Chemicals, 5%, 5 mL), and then agitated to produce a silver NP solution. Hydrazine monohydrate (Wako Chemicals, 98%, 6 mL) was added to the solution as a reducing agent, and the glass substrate was simultaneously dipped into it at 25°C. Silver NPs deposited on the substrate surface. Depending on the time, silver NP layers with various geometries were formed on the substrate. The substrate was then removed, rinsed in DI water, and dried under N_2 gas. By this process, silver NPs approximately 30 nm in diameter were deposited on the glass surface.

2.2 *Forming gold/silver NPs*

Gold/silver NP hetero-nanostructures were fabricated using the above two liquid-phase reduction processes, as shown in Fig. 1. The surface of the glass substrate was modified with APTS to deposit the gold NPs. After a designated amount of gold NPs was formed on the surface, the APTS layer was removed with an oxygen plasma at 50 W for 0.5 s. Subsequently, the substrate underwent the modified silver mirror reaction to deposit silver NPs. As a result, gold and silver NPs, approximately 10 and 30 nm in diameter, respectively, formed nanostructures on the glass substrate.

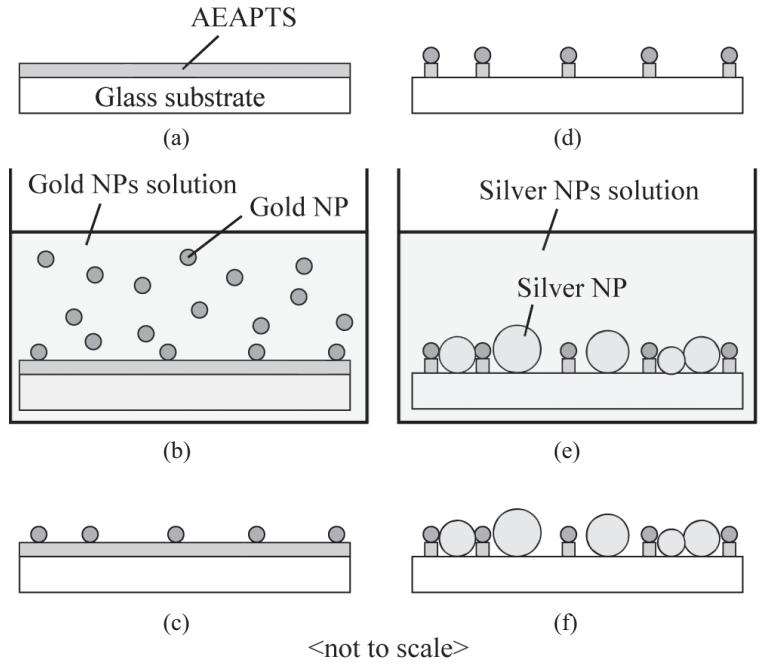

Fig. 1. Fabrication of gold/silver hetero-nanostructure substrates.

2.3 *Fluorescence enhancement measurement*

We investigated fluorescence enhancement using 10 μL of 100 nM rhodamine-6G (R6G) samples in ethanol. Samples were prepared by dropping the dye solution on the respective glass substrate, which was then immediately covered with a cover glass. Spectra of the substrates were recorded with excitation at an incident angle of 45°, and fluorescence collection at 22.5° to reduce the amount of reflection. Fluorescence emission spectra with wavelengths over the range of 540–700 nm were acquired using an excitation wavelength of 520 nm (Fluorolog-3 spectrophotometer, Horiba Jobin Yvon). The spectral width was set to 4 nm. Both the excitation and emission slit widths were set to 4 nm.

3. Results and Discussion

3.1 *Deposition of metal NPs*

Dense, uniform silver NPs were successfully formed on a glass substrate, with the most uniform silver NP layer formed at a reaction time of 80 s. This result was consistent with that of a previous work and the diameters of the silver NPs were 30± 7.3 nm.[25] The number of silver NPs on the glass substrate increased with increasing

reaction time. The NPs were not dispersed, but formed island structures while growing into a thin film.

Gold NPs were also successfully deposited on an APTS-modified glass substrate, as shown in Fig. 2(a). The reaction time was 6 h. The particle size distribution was obtained from 300 individual particles, and was 10.5±2.2 nm in diameter, as shown in Fig. 2(b). Unlike silver NPs, the gold NPs were dispersely deposited, and formed a single layer. The interparticle distance measured by FE-SEM decreased from 201 to 28 to 16 nm on average as the reaction time increased from 10 min to 1 to 6 h, as shown in Fig. 3. The area ratio, which is the ratio of the area occupied by gold NPs to the entire substrate area, increased with increasing reaction time (Fig. 3), but we did not observe any variation in the gold NP size with respect to reaction time.

3.2 *Gold/silver NP substrates*

We investigated the effect of the presence of gold NPs on the deposition of silver NPs. We fixed the reaction time of silver NPs to 40 s, at which silver NPs would occupy about half of the area, and varied the reaction time for the gold NPs, from 10 min to 1 to 6 h. Figure 4 shows SEM images of gold/silver NPs. Given the differences in the size distributions of silver and gold NPs, we could roughly differentiate between them on the basis of their size alone. When the gold NP reaction time was 10 min, given the small area ratio of gold NPs of 4% and the large interparticle distance of 200 nm, silver NPs formed island structures as they did without gold NPs present. At a gold NP reaction time of 1 h, dispersed silver NPs were deposited, and were isolated from each other. This was because the interparticle distance of gold NPs after 1 h of reaction time was 28

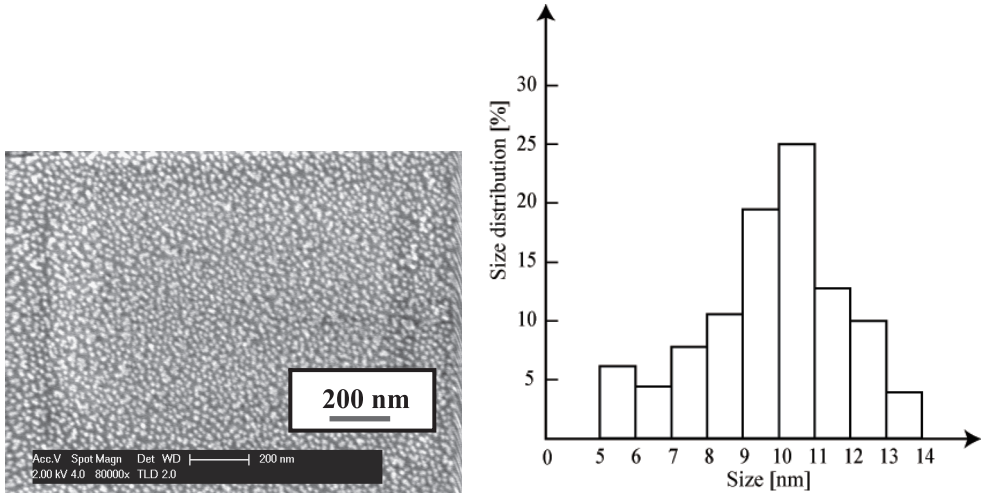

(a) (b)

Fig. 2. (a) SEM image and (b) size distribution of gold NPs on APTS-modified glass substrates.

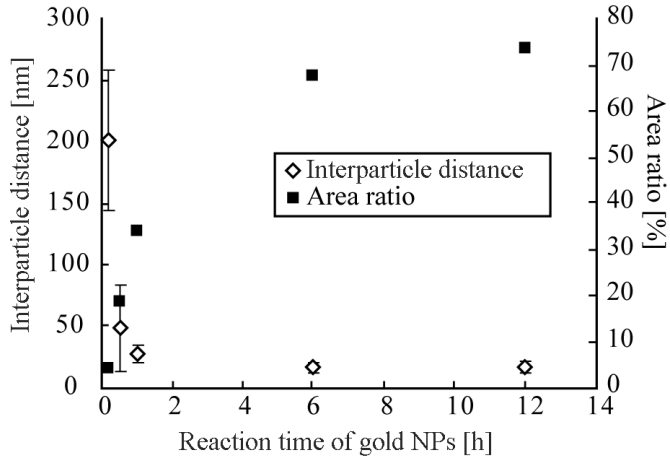

Fig. 3. Interparticle distance and area ratio of gold NPs at various reaction times.

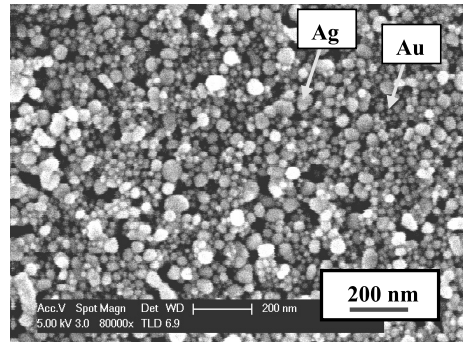

(a)

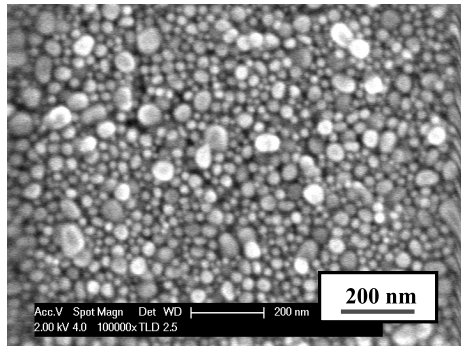

(b)

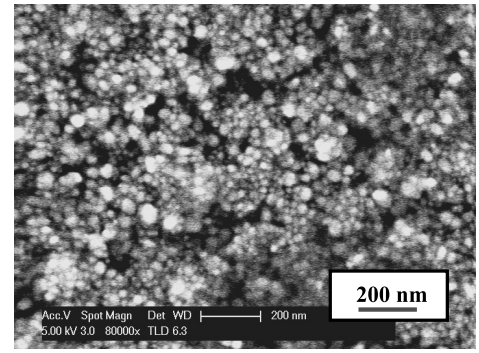

(c)

Fig. 4. SEM images of gold/silver NP substrates (reaction times: gold (a) 10 min, (b) 1 h, and (c) 6 h, silver 40 s).

nm, which was comparable to the size of the silver NPs. Silver NPs filled the gaps in the gold NPs after 40 s of reaction time. When the gold NP reaction time was increased to 6 h, silver NPs were found to deposit on both the glass substrates and the gold NPs, to form island structures. This *posteriori* analysis is summarized in Fig. 5.

Figure 6 shows SEM images of gold/silver NP substrates, for which the gold NP reaction time was 1 h and the silver NP reaction time was varied. Since the area ratio of gold NPs after 1 h of reaction time was 34%, silver NPs filled the gaps between the gold NPs, forming a single layer after 40 s of reaction. In contrast, the silver NPs could not fill the gaps at a reaction time of 20 s, and overflowed the gaps to form an aggregated layer at a reaction time of 80 s.

Thus, various hetero-nanostructures of gold and silver NPs were successfully formed by controlling the reaction times. The most uniform single layer of gold and silver NPs was obtained using reaction times of 1 h and 40 s, respectively.

3.3 *Fluorescence enhancement*

We investigated the fluorescence enhancement of gold/silver hetero-nanostructure substrates using 100 nM R6G dye as a sample. The fluorescence spectra of R6G on pristine glass, silver NPs, gold NPs, and gold/silver NP substrates with different

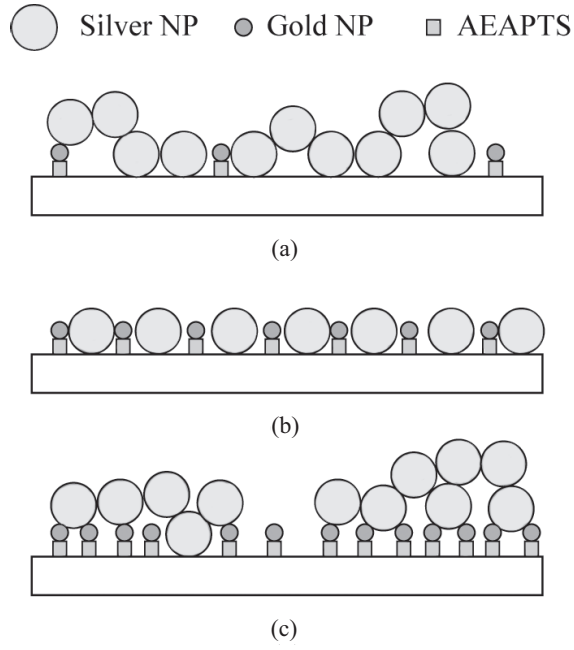

Fig. 5. Schematic illustration of the deposition of silver NPs on a gold NP/ glass substrate (reaction times: gold (a) 10 min, (b) 1 h, and (c) 6 h).

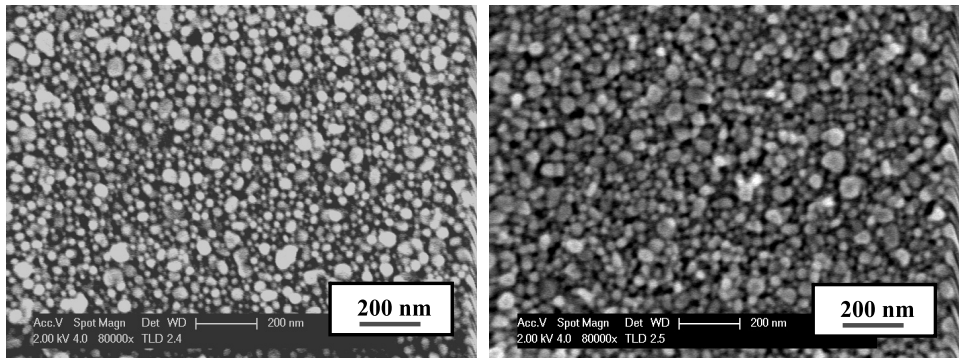

(a) (b)

Fig. 6. SEM images of gold/silver NP substrates (reaction times: gold 1 h, silver (a) 20 s, (b) 80 s).

composition ratios were acquired. We measured fluorescence signals from 5 randomly selected points on a substrate, and tested 3 substrates for each condition. Fluorescence spectra from the substrates (one substrate for each condition) are depicted in Fig. 7(a). The fluorescence intensities were enhanced by factors of 0.26, 4.0, and 9.5 on the gold NP, silver NP, and gold/silver NP substrate (gold and silver reaction times of 1 h and 40 s), respectively, compared with a pristine glass substrate. Gold NPs were reported to quench fluorescence,[35–38] in agreement with the results shown in Fig. 7(a). Silver NPs, however, enhanced the fluorescence signals. Figure 7(b) shows the fluorescence enhancement by silver NP and gold/silver NP substrates with respect to the reaction time of the silver NPs. The strongest enhancement of 8 on average was obtained from a substrate with a silver NP reaction time of 40 s and a gold NP reaction time of 1 h. Given that the densities of silver and gold NPs increased with the reaction time, the high enhancement when a silver NP reaction time was 40 s and a gold NP reaction time was 1 h was achieved not because the surface area and/or the density of silver NPs simply increased but because the substrate contained a favorable geometry at nanoscale. As discussed in § 3.2, under these conditions, isolated silver NPs formed on the substrate, densely filling the gaps between the gold NPs. This nanoscale geometry and the high density of silver NPs resulted in the strongest fluorescence enhancement.

Figure 7(a) shows the redshift of fluorescence spectrum of the gold/silver NP substrate by 8 nm. The redshift in surface-enhanced fluorescence depended on the nanostructures exerting fluorescence enhancement.[39] LSPR of silver NPs was reported to depend on the nanostructures as well as the concentration of R6G.[40] We consider that the optical property of the silver/gold NP substrate was different from those of others and the apparent concentration of R6G on the substrate was higher than those of others owing to its higher fluorescence enhancement, which resulted in the reabsorption of fluorescence of R6G with short wavelengths and the redshift of the peak.

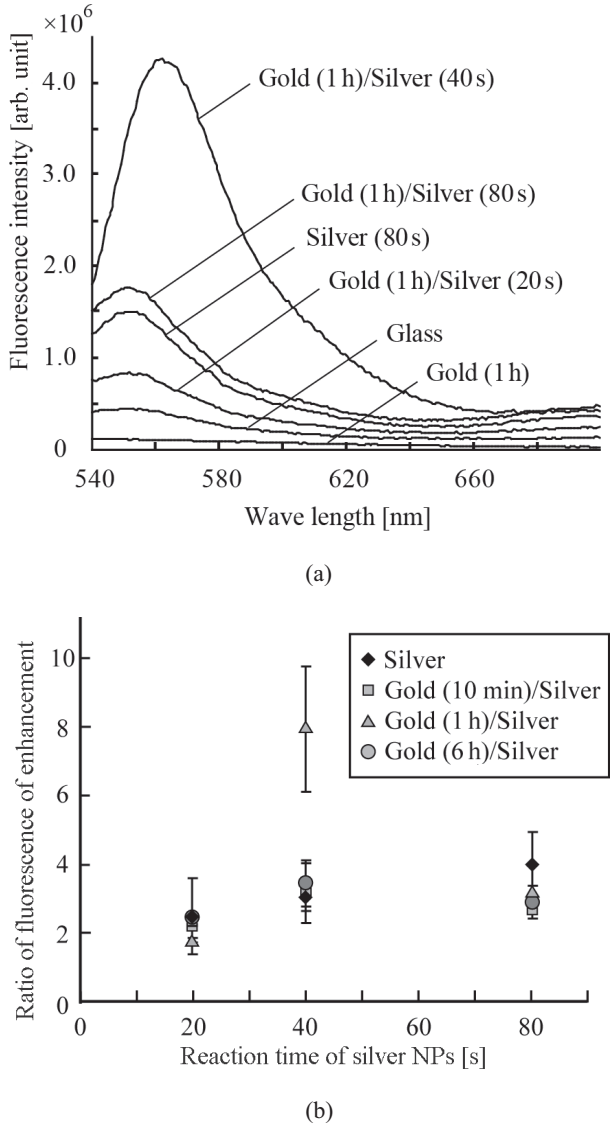

Fig. 7. (a) Fluorescence spectra of 100 nM R6G on glass, gold NP, silver NP, and gold/silver NP substrates. (b) The fluorescence was enhanced on the gold/silver NP substrate by a factor of 8 on average.

4. Conclusions

We developed a low-temperature, low-vacuum, bottom-up process of manufacturing nanostructures composed of silver/gold NPs. The process included surface modification of the glass substrate with an APTS SAM. Gold NPs regulated the deposition of silver NPs, causing the silver NPs to deposit as isolated NPs rather than as aggregated NPs. This enabled the gold/silver NP substrate to exhibit higher fluorescence enhancement than substrates with either only silver or only gold NPs. The proposed gold and silver nanoparticle substrates are readily applicable to promising NP applications, such as ultra-sensitive bio/chemical detection and catalysis.

Acknowledgement

This work was supported by the Ministry of Education, Culture, Sports, Science and Technology (MEXT), Grant-in-Aid for Scientific Research (S) (21226006).

References

1 T. Shtoyko, E. G. Matveeva, I.-F. Chang, Z. Gryczynski, E. Goldys and I. Gryczynski: Anal. Chem. **80** (2008) 1962.
2 P. P. Pompa, L. Martiradonna, A. D. Torre, F. D. Sala, L. Manna, M. De Vittorio, F. Calabi, R. Cingolani and R. Rinaldi: Nat. Nanotechnol. **1** (2006) 126.
3 K. Aslan, I. Gryczynski, J. Malicka, E. Matveeva, J. R. Lakowicz and C. D. Geddes: Curr. Opin. Biotechnol. **16** (2005) 55.
4 T. Nakamura and S. Hayashi: Jpn. J. Appl. Phys. **44** (2005) 6833.
5 F. Xie, M. S. Baker and E. M. Goldys: Chem. Mater. **20** (2008) 1788.
6 F. Xie, M. S. Baker and E. M. Goldys: J. Phys. Chem. B **110** (2006) 23085.
7 M. Moskovits: Rev. Mod. Phys. **57** (1985) 783.
8 H. X. Xu, J. Aizpurua, M. Kall and P. Apell: Phys. Rev. E **62** (2000) 4318.
9 K. Kneipp, Y. Wang, H. Kneipp, I. Itzkan, R. R. Dasari and M. S. Feld: Phys. Rev. Lett. **76** (1996) 2444.
10 K. Kneipp, Y. Wang, H. Kneipp, L. T. Perelman, I. Itzkan, R. R. Dasari and M. S. Feld: Phys. Rev. Lett. **78** (1997) 1667.
11 K. Kneipp, H. Kneipp, V. B. Kartha, R. Manoharan, G. Deinum, I. Itzkan, R. R. Dasari and M. S. Feld: Phys. Rev. E **57** (1998) R6281.
12 K. Kneipp, H. Kneipp, I. Itzkan, R. R. Dasari and M. S. Feld: Chem. Rev. **99** (1999) 2957.
13 M. Moskovits: J. Raman Spectrosc. **36** (2005) 485.
14 Y. Fujiwara, Y. Kobayashi, K. Kita, R. Kakehashi, M. Noro, J. Katayama and K. Otsuka: J. Electrochem. Soc. **155** (2008) D377.
15 S. P. Ramnani, S. Sabharwal, J. V. Kumar, K. H. P. Reddy, K. S. R. Rao and P. S. S. Prasad: Catal. Commun. **9** (2008) 756.
16 K. Tsujino and M. Matsumura: Electrochim. Acta **53** (2007) 28.
17 S. Chakraborty and C. R. Raj: Biosens. Bioelectron. **24** (2009) 3264.
18 G. A. Somorjai and J. Y. Park: Top. Catal. **49** (2008) 126.
19 Y.Yamamoto, S. Takeda, H. Shiigi and T. Nagaoka: J. Electrochem. Soc. **154** (2007) D462.
20 K. Fujiwara, H. Watarai, H. Itoh, E. Nakahama and N. Ogawa: Anal. Bioanal. Chem. 386 (2006) 639.

21 S. Pramanik, P. Banerjee, A. Sarkar and S. C. Bhattacharya: J. Lumin. **128** (2008) 1969.
22 X. Ji, X. Song, J. Li, Y. Bai, W. Yang and X. Peng: J. Am. Chem. Soc. **129** (2007) 13939.
23 L. Qu and L. Dai: J. Phys. Chem. B **109** (2005) 13985.
24 D. Yu and V. W.-W. Yam: J. Phys. Chem. B **109** (2005) 5497.
25 K. Hanada, K. Kurooka and N. Miki: Sens. Mater. **21** (2009) 129.
26 R. F. Aroca and C. J. L. Constantino: Langmuir **16** (2000) 5425.
27 C. J. L. Constantino, T. Lemma, P. A. Antunes and R. Aroca: Anal. Chem. **73** (2001) 3674.
28 C. J. L. Constantion, T. Lemma, P. A. Antunes and R. Aroca: Spectrochim. Acta, Part A **57** (2001) 281.
29 K. Esumi, T. Matsumoto, Y. Seto and T. Yoshimura: J. Colloid Interface Sci. **284** (2005) 199.
30 M. S. Chen and D. W. Goodman: Catal. Today **111** (2006) 22.
31 R. I. Nooney, O. Stranik, C. McDonagh and B. D. MacCraith: Langmuir **24** (2008) 11261.
32 A. K. Sinha, S. Seelan, S. Tsubota and M. Haruta: Top. Catal. **29** (2004) 95.
33 E. G. Matveeva, I. Gryczynski, A. Barnett, Z. Leonenko, J. R. Lakovics and Z. Gryczynski: Anal. Biochem. **363** (2007) 239.
34 S. S. Shankar, L. Rizzello, R. Cingolani, R. Rinaldi and P. P. Pompa: ACS Nano **3** (2009) 893.
35 S. K. Ghosh, A. Pal, S. Kundu, S. Nath and T. Pal: Chem. Phys. Lett. **395** (2004) 366.
36 G. Schneider, G. Decher, N. Nerambourg, R. Praho, M. H. Werts and M. Blanchard-Desce: Nano Lett. **6** (2006) 530.
37 S. A. Levi, A. Mourran, J. P. Spatz, F. C. J. M. van Veggel, D. N. Reinhoudt and M. Moller: Chem. Eur. J. **8** (2002) 3808.
38 K. Aslan, S. N. Malyn and Ch. D. Geddes: J. Fluoresc. **17** (2007) 7.
39 P. J. Tarcha, J. Desaja-Gonzalez, S. Rodriguez-Llorente and R. Aroca: Appl. Spectrosc. **53** (1999) 43.
40 J. Zhao, L. Jensen, J. Sung, S. Zou, G. C. Schatz and R. P. Van Duyne: J. Am. Chem. Soc. **129** (2007) 7647.